

Seismic Modeling 1: Anisotropy

Tuesday Morning

Three-Dimensional Wave Propagation Simulation in Elastic–Anisotropic Media

SM 1.1

Dan Kosloff, Tel-Aviv University, Israel; Jose M. Carcione, Bjorn Rommel, and Alfred Behle, Hamburg University, West Germany

SUMMARY

This work presents a new scheme for wave propagation simulation in three-dimensional elastic-anisotropic media. The modeling is based on the rapid expansion method (REM) as time integration algorithm, and the Fourier pseudospectral method for computation of the spatial derivatives. The modeling allows arbitrary elasticities and density in lateral and vertical directions.

Numerical methods which are based on finite-difference techniques (in time and space) are not efficient when applied to realistic 3-D models, since they require considerable computer memory and time to obtain accurate results. On the other hand, the Fourier method permits a significant reduction of the working space, and the REM algorithm gives machine accuracy with the same computational effort as the usual second-order temporal differencing scheme.

The modeling scheme was implemented on a CONVEX vector computer. Due to memory limitations the example presented in this work is restricted to the problem of wave propagation in a homogeneous transversely-isotropic medium, although the computer code is available for the computation of snapshots and synthetic seismograms in heterogeneous models, and for the use in parallel computers like for instance the CRAY X-MP system.

INTRODUCTION

The growing importance of 3-D seismic surveys requires the development of an elastic-anisotropic forward modeling code for an appropriate interpretation of the results. For instance, of importance to global seismology is the study of the Earth's crust and upper mantle, which are known to be anisotropic; 3-D polarization analysis in anisotropic media can be used as structure indicator: shear wave splitting gives information about the alignment of cracks, an important parameter in reservoir engineering (Crampin, 1985).

The proposed approach is based on spectral methods, both in space and time, and therefore wave field computations are highly accurate. Besides this fact, vectorization (mainly the FFT routine) and parallelization of the algorithm provides a very efficient scheme in terms of computer time.

The program has been written to compute snapshots and synthetic seismograms in a general anisotropic medium, which can be described by 21 independent parameters. The modeling code provides different types of seismic sources: directional forces, and purely compressional and shear initial motions, with causal zero phase Ricker, Gaussian and vibrator wavelets. In addition with the possibility of simulating a free surface, these features enable the modeling of a variety of seismic surveys.

EQUATION OF MOTION

In a three-dimensional continuous medium the linearized equations of momentum conservation are

$$\rho \ddot{u}_i = \frac{\partial \sigma_{ij}}{\partial x_j} + \rho f_i, \quad i = 1, 2, 3 \quad (1)$$

where x_j are Cartesian coordinates, $\sigma_{ij}(\vec{x}, t)$ are the stress components, $u_i(\vec{x}, t)$ are the displacements, $\rho(\vec{x})$ denotes the density, and $f_i(\vec{x}, t)$ are the body forces. Repeated indices imply summation and a dot above a variable indicates time differentiation.

The constitutive relation is given by

$$\vec{T} = C \vec{E}, \quad (2)$$

where

$$\vec{T}^T = [\sigma_{11}, \sigma_{22}, \sigma_{33}, \sigma_{23}, \sigma_{13}, \sigma_{12}], \quad (3)$$

is the stress vector,

$$\vec{E}^T = [\epsilon_{11}, \epsilon_{22}, \epsilon_{33}, 2\epsilon_{23}, 2\epsilon_{13}, 2\epsilon_{12}], \quad (4)$$

is the strain vector, with $\epsilon_{ij}(\vec{x}, t)$ the strain components given by

$$\epsilon_{ij} = \frac{1}{2} \left(\frac{\partial u_i}{\partial x_j} + \frac{\partial u_j}{\partial x_i} \right), \quad i, j = 1, 2, 3 \quad (5)$$

The superscript 'T' denotes transposed. The elasticity matrix $C(\vec{x})$ is symmetric with c_{IJ} , $I, J = 1, \dots, 6$ arbitrarily space-dependent.

The REM algorithm requires that the equation of motion be written as

$$\ddot{\vec{u}} = -L^2 \vec{u} + \vec{f}, \quad (6)$$

where \vec{u} is the displacement vector, \vec{f} is the vector of the body forces, and $-L^2$ is a linear operator which contains the spatial derivatives and the material parameters. This matrix operator is expressed by

$$-L^2_{ij} = \frac{1}{\rho} G_{iJ} c_{JK} G_{Kj}^T, \quad i, j = 1, 2, 3 \quad J, K = 1, \dots, 6 \quad (7)$$

with

$$G = \begin{bmatrix} \frac{\partial}{\partial x_1} & 0 & 0 & 0 & \frac{\partial}{\partial x_3} & \frac{\partial}{\partial x_2} \\ 0 & \frac{\partial}{\partial x_2} & 0 & \frac{\partial}{\partial x_3} & 0 & \frac{\partial}{\partial x_1} \\ 0 & 0 & \frac{\partial}{\partial x_3} & \frac{\partial}{\partial x_2} & \frac{\partial}{\partial x_1} & 0 \end{bmatrix}. \quad (8)$$

After spatial discretization, equation (6) becomes a coupled system of differential equations for the displacements at the nodes of the numerical mesh. Like the Chebychev spectral method (Carcione et al., 1988), the REM algorithm is based on a modified expansion of the formal solution of equation (6), in terms of Chebychev polynomials. A detailed description of the REM algorithm with comparison to second order temporal differencing can be found in Edwards et al., (1987) and Kosloff et al., (1989).

NUMERICAL SIMULATION

Practical applications of 3-D forward modeling require important quantities of CPU memory. Typical problems need tens of megawords of storage, a size which exceeds the central memory of most computer systems. To test the present algorithm we use a CONVEX computer system with 8 megawords of central memory. Due to this limitation we consider wave propagation in a transversely-isotropic solid which require much less memory than a general anisotropic medium.

Implementation of the REM algorithm needs three times the number of displacements components at each grid point, three additional arrays for temporal storage, plus the arrays for the elasticities and density, i.e., $M = 15$ for the isotropic case, $M = 18$ for the transversely isotropic case, and $M = 34$ for the general anisotropic case. Total memory requirements are given by $MN_XN_YN_Z$ million words, a quantity that should not exceed the CPU memory to have efficient performances. N denotes number of grid points.

The example considers wave propagation in a homogeneous transversely isotropic medium whose symmetry axis coincides with the vertical axis (Z -axis). The material is defined by the elasticities, $c_{11} = 66.6GPa$, $c_{12} = 19.7GPa$, $c_{13} = 39.4GPa$, $c_{33} = 39.9GPa$ and $c_{44} = 10.9GPa$, and density $\rho = 2590Kg m^{-3}$, which represent Mesaverde clayshale (Thomsen, 1986). Figure 1 displays a section of the wave surfaces through a plane containing the symmetry axis. Modes qP and qSV are coupled while SH is pure. 3-D wave surfaces show azimuthal symmetry.

Parameters of the numerical mesh are $N_X = N_Y = N_Z = 75$, with $DX = DY = DZ = 25m$, the grid size. The motion is initiated by an X -directional force having a causal time function with $20Hz$ dominant frequency. Figure 2 displays snapshots after $t = 0.228s$ in XY , XZ and YZ -planes, through the source position and at $325m$ from this position; Z -axis is always vertical, in XY -planes Y -axis is vertical. Some characteristics shall be discussed. If we define the incidence plane by the propagation direction and the Z -axis, qP and qSV motion lie in this plane, while SH motion is normal to the plane. Hence, the u_x -component does not contain SH motion.

In-source planes: XY -plane: by isotropy wave surfaces sections are circles; u_x and u_y components show mainly qP and SH motion, and qSV motion around the line $Y = 0$. This is a contribution from the slower branches of the qSV mode for which the wavenumber vector is not parallel to the line $Y = 0$. XZ -plane: the u_x -component has only qP and qSV motions since SH motion is normal to the plane, although by symmetry the u_y -component is zero. The cusps can be distinguished. The small contribution of SH motion in the u_x -component is due to the uncertainty in the position of the source and the recording plane. The uncertainty is given by the grid size. YZ -plane: SH motion is normal to this plane. The characteristic ellipse can be seen in the u_x -component. There is a strong contribution from the qSV mode around the line $Y = 0$ since the Green's function in the symmetry axis presents a singularity in the second arrival (see Carcione et al., 1988). This contribution is not present in the isotropic case. Off-source planes contain the three wave motions except the SH in the u_x -component as mentioned before.

Figure 3 shows synthetic seismograms. Coordinates are relative to the source position; (a) only SH motion; (b) qP and SH motion. Anisotropy is manifested in the different slopes of the SH event in (a) and (b); (c) mainly SV motion and small qP .

ACKNOWLEDGEMENTS

Part of this work was supported by a '3-D modeling' project under contract 03E-6424-a of the BMFT, West Germany, and contract EN3C-0008-D of the Commission of the European Communities. One of us (J.M.C.) has been aided by an Alexander von Humboldt Fellowship.

REFERENCES

- Carcione, J.M., Kosloff, D., and Kosloff, R., 1988, Wave propagation simulation in an elastic (transversely isotropic) medium: Q. J. Mech. Appl. Math.; 41, 319-345.
- Crampin, S., 1985, Evaluation of anisotropy by shear-wave splitting: Geophysics, 50, 142-152.
- Edwards, M., Kosloff, D., Reshef, M., Tessmer, E., 1987, Three dimensional solutions of the equations of dynamic elasticity by a new rapid expansion method (REM): SEG abstracts, 57th Annual Meeting.
- Kosloff, D., Queiroz Filho, A., Tessmer, E., and Behle, A., 1989, Numerical solutions of the acoustic and elastic wave equations by a new rapid expansion method: Geophys. Prosp., in press.
- Thomsen, L., 1986, Weak elastic anisotropy: Geophysics, 51, 1954-1966.

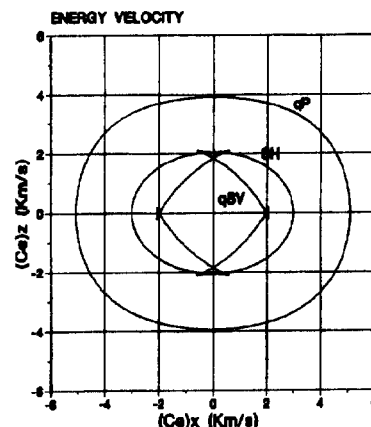


FIG. 1. Section of wave surfaces through a plane containing symmetry axis.

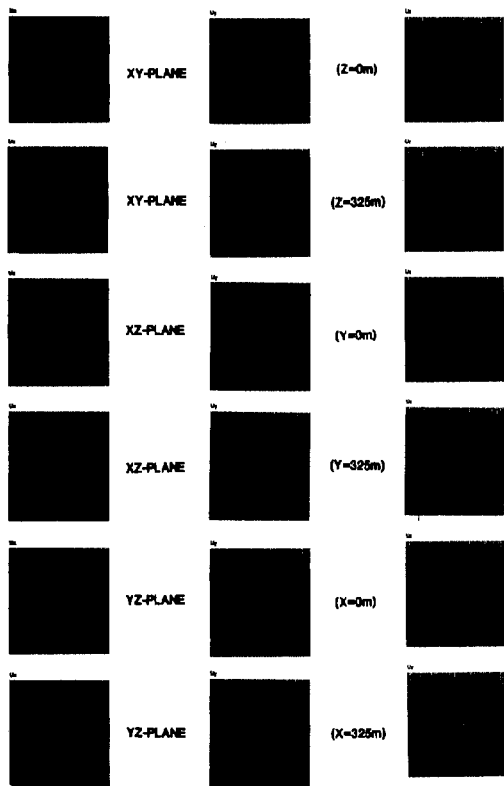
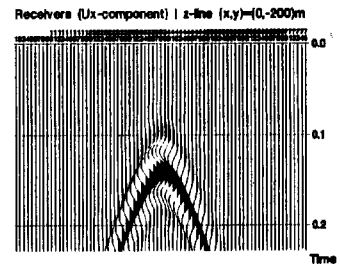
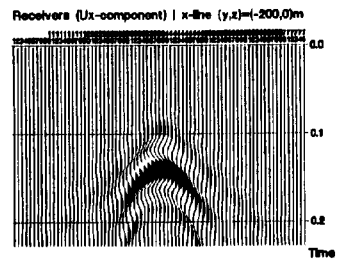


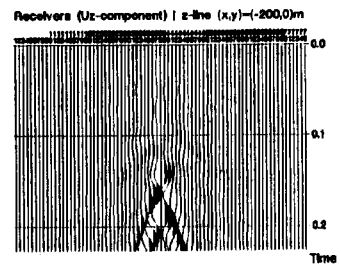
FIG. 2. Snapshots of wave field at several planes.



(a)



(b)



(c)

FIG. 3. Synthetic seismograms showing different wave modes.